Electrodeformation, Electroporation, and Electrofusion of Giant Unilamellar Vesicles

Rumiana Dimova and Karin A. Riske

Contents

Abstract

This chapter summarizes a spectrum of phenomena observed on model membranes exposed to electric fields. The considered model membrane system is giant unilamellar vesicles with sizes in the range of tens of microns. Because of their large size, the response of the membrane to electric fields can be directly visualized under the microscope. The membrane behavior is exemplified by

R. Dimova (✉)
Department of Theory and Bio-Systems, Max Planck Institute of Colloids and Interfaces, Potsdam, Germany
e-mail: dimova@mpikg.mpg.de

K.A. Riske
Departamento de Biofísica, Universidade Federal de São Paulo, São Paulo, Brazil
e-mail: kariske@unifesp.br

D. Miklavcic, *Handbook of Electroporation*,
DOI 10.1007/978-3-319-26779-1_199-1

several types of responses: First, the vesicles undergo morphological changes and adopt prolate, oblate, or spherocylindrical shapes. In general, the vesicle morphology depends on the conductivity conditions of the immersion and encapsulated solutions, and in the case of alternating fields – on the field frequency. Second, after switching the electric field off, these shapes can relax back to a sphere. The relaxation times depend on the initial membrane tension and on the reached transmembrane potential. Third, the vesicles can undergo topological changes such as formation of pores and, in the case of vesicles in contact, fusion. All these processes depend on the material characteristics of the membrane such as mechanical (bending rigidity and stretching elasticity), rheological (membrane shear surface viscosity), and electrical (capacitance) properties of the lipid bilayer. This chapter gives an overview of these properties and their dependence on the membrane phase state, and presents approaches for directly assessing them using giant unilamellar vesicles.

Keywords

Giant unilamellar vesicles • Model membranes • Membrane mechanical properties • Vesicle deformation • Poration • Membrane fusion

Introduction

The effects of electric fields on cells have long been a subject of interest and exploration. The lipid bilayer of the plasma cellular membrane acts as an electric insulator so that a variety of electrical phenomena take place when cells are exposed to electric fields, of either alternating (AC) or direct current (DC). AC fields, for instance, are known to induce cell deformation, reorientation, and movement, in some cases leading to cell alignment. Strong fields, usually applied as single or consecutive DC pulses, can lead to the phenomenon of electroporation, also referred to as electropermeabilization or electrical breakdown, whereby (transient) pores open across the cellular membrane. Electroporation has obvious applications when the target is to insert exogenous molecules into the intracellular medium, as is the case, for instance, in gene therapy ("▶ Gene Delivery by Electroporation In Vitro: Mechanisms," "▶ Molecular Transmembrane Transport with Giant Unilamellar Vesicles (GUVs)," and "▶ Nucleic Acid Electrotransfer in Mammalian Cells: Mechanistic Description"). When cells in contact are electroporated they can fuse and mix their intracellular compartments and plasma membrane (a process known as hybridization), which also finds a large range of applications.

To better understand the mechanistic details underlying electrical phenomena in cells, model systems, mainly lipid vesicles, have been widely employed. Lipid vesicles are handy tools to explore all sorts of membrane-related biological phenomena, especially those in which the lipid phase of the biological membrane plays a key role. That is certainly the case when regarding the effects of electric fields on cells. Electric field-induced vesicle shape deformation, movement, permeabilization, and fusion have been investigated for several decades already,

and a large body of information has been collected on this topic. It has become obvious that the response of the lipid vesicles to electric fields is defined by the membrane material properties, such as softness, fluidity, ability to be stretched/compressed, electrical capacitance, and surface viscosity. Of special relevance to vesicle studies are giant unilamellar vesicles (GUVs) , cell-sized objects which can be individually and directly observed with an optical microscope. GUVs have been widely used in this research area, with the clear size advantage over their counterparts, the conventional large or small unilamellar vesicles with sizes between tens and hundreds of nanometers.

The study of GUVs in the presence of electric fields has two main purposes. On the one hand, the mechanistic details of cell deformation, permeabilization, and fusion can be understood and used in the development of new protocols for biotechnological and biomedical applications. On the other hand, electric fields can be used to manipulate GUVs for the purpose of helping the investigation of membrane phenomena and/or to impose a well-controlled external perturbation with the aim of extracting material properties of lipid bilayers of different compositions and in different conditions of biological relevance.

The chapter is organized as follows. First, the use of GUVs as biomimetic model for deducing membrane properties are introduced, focusing on their response to electric pulses. Then, three different field-induced effects are discussed in detail: vesicle deformation, poration, and fusion.

Giant Unilamellar Vesicles as Model Systems to Study Membrane Properties

Lipid vesicles, also called liposomes, have often been used as mimetic models for the complex biological membrane because they are easy to prepare and handle, and their lipid composition can be precisely controlled and varied. Depending on the preparation method, lipid vesicles can be unilamellar (one bilayer encapsulating internal volume) or multilamellar (made of several bilayers) and of definite size, ranging from tens of nanometers to tens of micrometers. This chapter will focus on the largest ones, called giant unilamellar vesicles or GUVs which are cell-sized objects of typical diameter around 10–50 μm. They can be easily visualized under an optical microscope. GUVs have several advantages over the conventional small liposomes (usually with diameters of the order of 100 nm). Giant vesicles exhibit nearly zero membrane curvature, thus better mimicking the conditions of the plasma membrane, and can be individually manipulated and observed. In the last decades, GUVs have become a well-established platform on which membrane properties can be quantified and many membrane-related phenomena, such cell adhesion, curvature sensing or generation, membrane fusion, phase separation and domain formation, and effects of anchored or inserted molecules, can be studied. Additionally, membrane proteins can also be reconstituted in GUVs, thus allowing the investigation of protein functions and mobility.

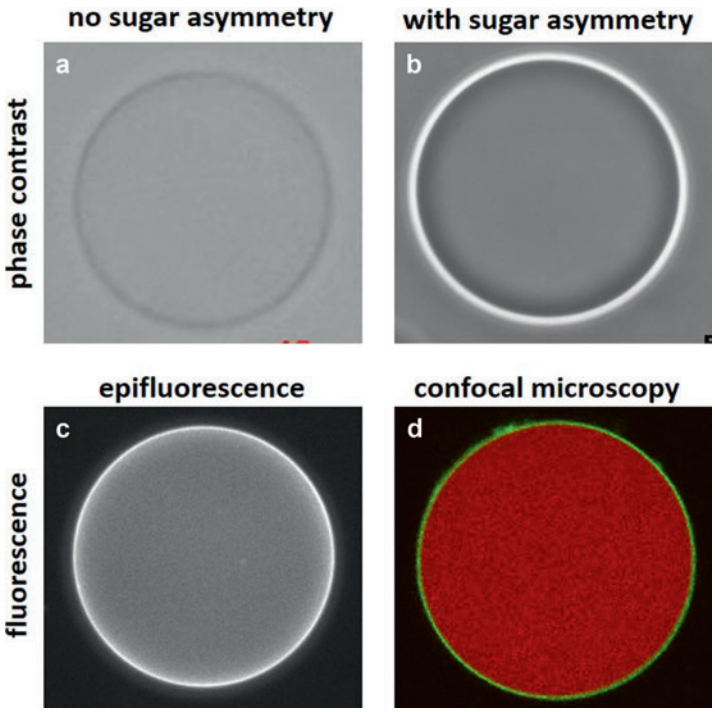

Fig. 1 *Top*: GUVs observed with phase contrast mode without (**a**) and with (**b**) sucrose/glucose in/out asymmetry. *Bottom*: GUVs observed with fluorescence-based microscopy whereby either the membrane is labeled and the vesicle is observed with epifluorescence (**c**) or both; the membrane and the solution encapsulated in the vesicle are labeled (in *green* and *red*, respectively) and observed with confocal microscopy (**d**). The dimeters of the GUVs are about 20–60 μm

Preparation and Observation of Giant Vesicles

GUVs are commonly prepared with the conventional electroformation method, although several other protocols have been described that allow formation of GUVs with a variety of lipids and growing media; for an overview of several commonly used methods consult (Walde et al. 2010). To observe GUVs with optical microscopy, transmission-light and fluorescence-based techniques are usually employed. Among the transmission-light techniques, the most commonly used are phase contrast, differential interference contrast (DIC), reflection interference contrast microscopy (RICM), and wide-field microscopy. Fluorescence-based microscopy includes e.g., epifluorescence, confocal microscopy, and total internal reflection fluorescence (TIRF) microscopy. In this case, to allow observation, fluorescent dyes have to be added, either to the membrane (typically ~0.5 mol% fluorescent molecules or fluorescently labeled lipids) or to the aqueous solution (water soluble probes added either internally or externally to the vesicles). Figure 1 shows representative images of GUVs observed with phase contrast,

epifluorescence, and confocal microscopy. The vesicles are very often prepared in a solution containing sucrose (with concentration typically in the range 0.1–0.2 M) and dispersed in an isoosmolar solution with glucose. This creates a sugar asymmetry that enhances the optical contrast in phase contrast mode (see Fig. 1a, b) and stabilizes the vesicles onto the bottom of the observation chamber due to gravity. The asymmetry of sugars and of water soluble fluorescent dyes between the inner and outer medium can be used to report on membrane permeability, since this asymmetry between the inner and outer vesicle compartments is only maintained as long as the membrane remains impermeable to sucrose/glucose and to the fluorescent molecule. In the latter case, probes of different sizes can be used so that the pore size can be estimated.

Bilayer Phases

Depending on the constituent lipids and the temperature, membranes can be found in different phases or even exhibit lateral phase separation. Single-component bilayers are either in a gel or fluid phase, depending on the temperature. At room temperature, unsaturated lipids are often in a fluid phase, also called liquid-disordered phase, characterized by large lateral mobility and chain disorder. Long and saturated chains at room temperature are usually in a gel, or solid, phase, with chains that are tightly packed and ordered and with virtually no lateral mobility. Binary mixtures of lipids with cholesterol can be found in a liquid-ordered phase, in which the hydrocarbon chains are ordered but the lipids still exhibit large lateral mobility. Ternary and more complex mixtures can exhibit lateral phase coexistence. The biological membrane is mainly in the fluid phase, since most of its phospholipids have unsaturated chains but submicron domains resembling the liquid-ordered phase are postulated to transiently form and to perform important tasks, as signaling and endocytosis (Simons and Ikonen 1997). These nanodomains, the so-called membrane rafts, are rich in sphingomyelin (a long saturated lipid), cholesterol, and certain membrane proteins. Depending on composition and temperature, GUVs can be in the liquid-disordered, liquid-ordered, and gel phase or exhibit coexistence phases (typically, up to three phases can be simultaneously visualized). To visualize phase coexistence, fluorescently labeled lipids with known preference for one of the phases are used so that micron-sized domains can be distinguished with fluorescence microscopy. This chapter will predominantly discuss the properties of fluid membranes but some information on other phases will be included as well.

Mechanical and Rheological Properties of Bilayers

Simplistically, lipid bilayers may be viewed as a single ~5-nm thick film, which may be bent, compressed/stretched, and sheared (see Fig. 2 for a schematic illustration). Fluid membranes are very soft and flexible, because their bending elasticity modulus, κ, is only on the order of several k_BT, where k_BT is the thermal energy (Dimova

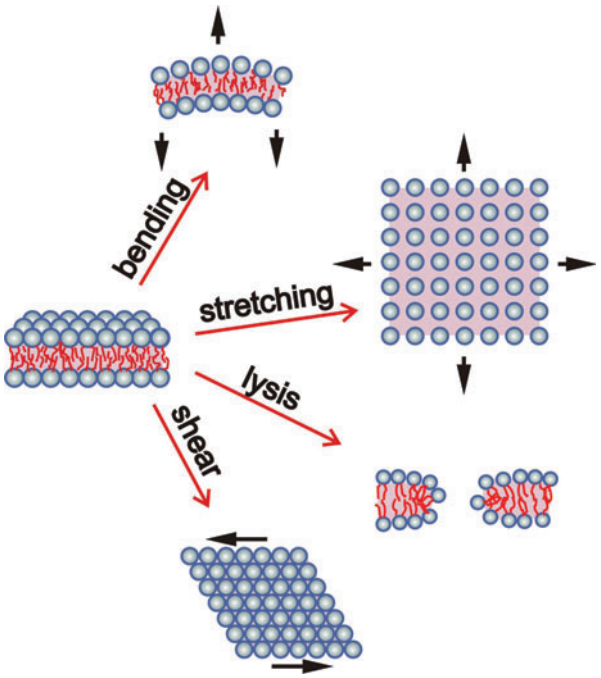

Fig. 2 Modes of bilayer membrane deformations: the response of the membrane to out-of-plane deformations is defined by the bending rigidity; response to lateral stretching is characterized by the stretching elasticity modulus; above certain threshold (lysis tension), the membrane can rupture, pore formation being one example of this process; lateral in-plane displacement is characterized by the shear surface viscosity

2014). Thus, fluid membranes exhibit thermal shape fluctuations that can be directly observed on tensionless GUVs under the microscope. When tension is applied to the membrane and gradually increased, one first pulls out the bilayer fluctuations and then eventually stretches the membrane on the molecular level, by changing the area per lipid molecule. The stretching elasticity modulus of lipid bilayers, K_a, is on the order of that of a rubber sheet with the same thickness, i.e., approximately 200–300 mN/m (Rawicz et al. 2000). Upon stretching, the lipid bilayer can sustain tensions up to about several mN/m (corresponding to about 5 % area increase). At certain critical tension, also known as the lysis tension, σ_{lys}, the membrane ruptures and pores open to relieve the stress. The energy penalty to form curved pore rims (hydrophilic pores) depends on the line (or edge) tension, γ, which is usually high for phospholipids, so that pores tend to eventually close and restore a bilayer structure. The resistance to shear in fluid membranes is negligible because they are thin. But the membrane and the surrounding fluid impose a hydrodynamic drag to the motion of an inclusion in the membrane, characterized by the membrane surface viscosity, η_s. Another important parameter to quantify membrane fluidity is the lateral diffusion coefficient, D, of lipids. In Table 1, some typical values of the constants discussed above are given for fluid-phase membranes. Note that the presence of cholesterol in fluid membranes will generally render a tighter and more ordered bilayer, with clear impact on all the properties reported. For comparison, some data on membranes in the gel phase are also given.

Table 1 Typical values of properties of membranes in different phase states

	Liquid-disordered	Liquid-ordered	Gel
Bending rigidity, κ	20 k_BT	100 k_BT	350 k_BT
Stretching elasticity, K_a	300 mN/m	1000 mN/m	
Lysis tension, σ_{lys}	5–10 mN/m	25 mN/m	
Surface viscosity, η_S	~10^{-8} N s/m	~10^{-7} N s/m	Diverges
Diffusion coefficient, D	~10^{-8} cm^2/s	~10^{-9} cm^2/s	<10^{-11} cm^2/s
Edge tension, γ	30 pN	150 pN	

Electrical Properties of Bilayers

Electric fields can cause a variety of effects on GUVs, most of which are also found in cells. The lipid bilayer can withhold a salt asymmetry and separate internal and external solutions of different conductivities and act as an insulator up to a certain degree. Free charges in solution move in response to the electric field and can accumulate at the membrane boundaries. The membrane then acts as a capacitor that charges with a characteristic time and acquires a transmembrane potential V_m, given by:

$$V_m = 1.5\, R\, E\, |\cos\theta|\, [1 - \exp(-t/t_c)] \tag{1}$$

where R is the vesicle radius, θ the tilt angle between the electric field direction and the surface normal, t is time, and t_c the charging time

$$t_c = RC_m\left(\frac{1}{\lambda_{in}} + \frac{1}{2\lambda_{ex}}\right) \tag{2}$$

with C_m being the membrane capacitance (~1 μF/cm^2) and λ_{in} and λ_{ex} the conductivities of the internal and external media, respectively. For low conductivity solutions (sugars only), the charging time $t_c \sim 500$ μs, and it decreases to a few μs when salt at millimolar concentration is present in the media.

The electric field induces a stress on the membrane, given by the Maxwell stress tensor. This leads to vesicle deformation and to an effective electrical tension σ_{el} which normally compresses the bilayer. At high tension, the bilayer eventually ruptures. This occurs above some critical transmembrane potential V_c, ("▶ Critical Electric Field and Transmembrane Voltage for Lipid Pore Formation in Experiments" and "▶ Critical Electric Field and Transmembrane Voltage for Lipid Pore Formation in Molecular Models") which is reached when the membrane undergoes lysis at tension $\sigma_{lys} = \sigma_o + \sigma_{el}$, where σ_o is the initial tension before the application of the electric field. For tensionless vesicles in the fluid phase ($\sigma_o \sim 0$), $V_c \sim 1$ V. However, V_c can be lower for vesicles that have some initial membrane tension (Riske and Dimova 2005). Vesicles in the liquid-ordered and gel phases are more resistant to electroporation, and V_c is higher. For the gel phase, V_c was reported to be around 10 V (Knorr et al. 2010). Above the poration threshold, electrical breakdown of the bilayer occurs and pores open to relieve the stress imposed on the membrane.

Electric fields can be of alternating (AC) and of direct (DC) current. AC fields applied to vesicles and cells are usually relatively moderate so that the poration threshold is not reached. The effects caused are then vesicle deformation (Dimova et al. 2007), lipid flow due to asymmetric field around the vesicle and dielectrophoresis, which can cause vesicle movement and pearl-chain formation in some field conditions. However, stronger AC fields (> 3 kV/m) are also able to induce poration (Harbich and Helfrich 1979). DC (usually square) pulses also induces vesicle deformation but can be set strong enough so as to reach the electroporation threshold and thus opening of pores (Riske and Dimova 2005). This has been largely employed to render cells transiently permeable ("▶ Pulsed Electric Fields Treatment of Biological Suspensions" and "▶ Electric Pulse Parameters Affecting Electroporation Treatment Outcome"). In GUVs, macropores of few micrometers open and can be visualized with optical microscopy (see ahead). After the pulse, these macropores usually close and the vesicle shape relaxes to its original shape. If GUVs in contact are porated, they can fuse. The dynamics of all these processes are governed by the material properties of the membranes as will be discussed on the following sections.

Experiments with GUVs in Electric Fields

Effects of electric fields on model membranes can be nicely illustrated and resolved using GUVs (Dimova et al. 2007; Dimova et al. 2009). On the one hand, GUVs have the dimensions of cells, so the typical field parameters are similar to those used in applications with cells. On the other hand, they can be individually observed and followed with video microscopy. Chambers with electrodes can be easily prepared using Pt-wires or adhesive copper tapes or can be purchased. The distance between the electrodes should be precisely known, so that the electric field can be calculated from the voltage applied between them. The examples shown in this chapter were obtained with a commercially available electrofusion chamber (Eppendorf, Germany) containing two Pt-wires of about 90 μm diameter and 500 μm apart. The lipid composition of the GUVs can be controlled and varied to allow quantification of membrane properties as a function of their composition. The results shown here were mainly obtained with unsaturated phosphatidylcholine (PC) lipids, either egg-PC or palmitoyloleoylphosphatidylcholine (POPC), thus with membranes in the fluid phase. In some cases, a fraction (up to 50 mol%) of the charged lipid palmitoyloleoylphosphatidylglycerol (POPG) was present to study the role of surface charges on the membrane properties.

Electrodeformation of GUVs

Vesicle Morphologies

Lipid vesicles are deformed by electric fields. AC fields induce ellipsoidal shape deformation which can be either prolate or oblate depending on the conductivity ratio ($\lambda_{in}/\lambda_{ex}$) between the inner and outer solutions and on the field frequency, ω

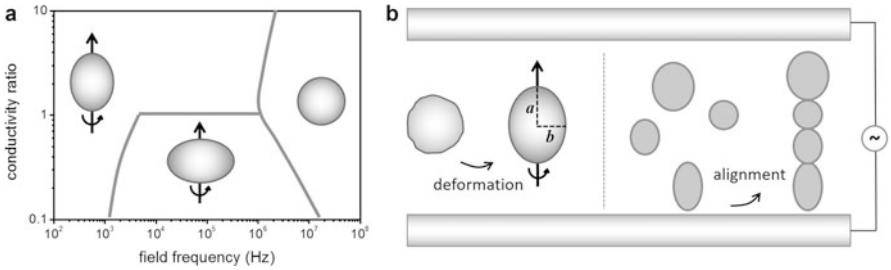

Fig. 3. (**a**) Morphological diagram of vesicle shape deformations induced by AC fields as a function of conductivity ratio $\lambda_{in}/\lambda_{ex}$ and field frequency ω. The symmetry axes of the prolate and oblate shapes are shown as *straight arrows*, and they align parallel with the electric field direction. (**b**) Some effects of AC fields. *Left*: vesicles with excess area stored in fluctuations are deformed and adopt prolate shapes (for $(\lambda_{in}/\lambda_{ex} > 1)$. The extent of vesicle deformation quantified by the aspect ratio *a/b* is related to the field strength and surface area and can be used to extract the bending stiffness of the membrane. *Right*: Due to dielectrophoresis, GUVs in AC fields move and align in pearl chains

(Aranda et al. 2008). In both cases, the symmetry axis of the ellipsoid shape is aligned with the electric field (the long axis in the case of prolates and the short one in the case of oblates). A representation of the morphological diagram of vesicle shapes induced as a function of the conductivity ratio $\lambda_{in}/\lambda_{ex}$ and the field frequency ω is shown in Fig. 3 (Aranda et al. 2008; Dimova et al. 2009). At very high field frequency ($\omega > 10^7$ Hz), the vesicles do not deform, because the field direction changes faster than the ions can respond to it. At lower frequencies and for $\lambda_{in}/\lambda_{ex} > 1$, the vesicles adopt prolate shapes. When the external conductivity is higher than that of the internal medium ($\lambda_{in}/\lambda_{ex} < 1$), a prolate-oblate shape transition occurs at $\omega \sim 10^3$ Hz. The critical frequency at which the vesicles undergo the prolate-oblate transition, together with the vesicle size and the conductivity ratio, can be used to extract the membrane capacitance. The extent of vesicle deformation depends on the field strength and on the vesicle excess area. Thus, AC fields of moderate strength (typically 200 V/cm) can be used to estimate the vesicle excess area stored in fluctuations from simple geometrical considerations of ellipsoidal shapes (prolate shape deformations are preferred because of the smaller deformation imposed by the chamber wall). Moreover, AC fields can be used to deduce the membrane bending stiffness, κ, by increasing the field strength and measuring the deformation induced in terms of the ratio between the vesicle semi-axes *a/b* and relating it to the imposed tension on the membrane (Gracià et al. 2010).

Moderate field frequencies (ω ~ 100 kHz) induce vesicle alignment as in a pearl chain due to dielectrophoresis, which can be helpful for bringing vesicles into contact and then study vesicle adhesion and/or fusion (see section "Electrofusion of GUVs").

DC pulses also induce vesicle deformation, but of transient nature, since the vesicle typically relaxes back to its original shape after the end of the pulse (Riske and Dimova 2005, 2006). Typical fields applied are square DC pulses of 0.5–5 kV/cm with duration of 0.05–5 ms, but nanosecond pulses of even higher strength have also been used. The examples that are discussed here were obtained with pulses of

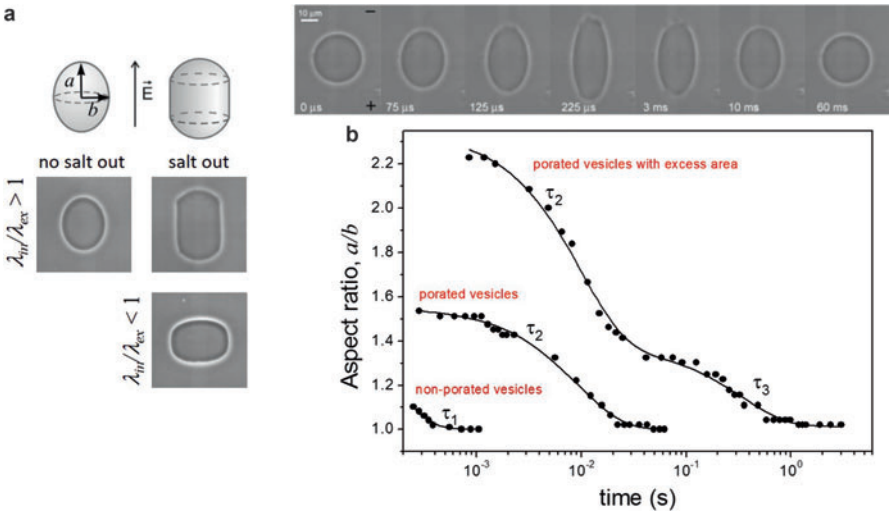

Fig. 4. (**a**) Shape deformations induced by DC fields. The cartoons show ellipsoidal and spherocylindrical shapes induced in the absence and presence of salt outside the vesicle, respectively. The images below are representative of the observed shapes as a function of conductivity ratio, $\lambda_{in}/\lambda_{ex}$, and presence of salt (~1 mM NaCl) (Adapted from Riske and Dimova (2006), Copyright 2006, with permission from Elsevier). (**b**) *Top*: representative sequence of an egg-PC GUV during and after application of a DC pulse (2 kV/cm, 200 µs) observed with a high temporal resolution ($\lambda_{in}/\lambda_{ex} > 1$, no salt out). The macropores can be visualized in the second, third, and fourth snapshots. *Bottom*: Time dependence of the aspect ratio *a/b* for three vesicles (nonporated, porated, and porated with excess area) and the respective relaxation characteristic times τ_1, τ_2, and τ_3 (pulse conditions: 1 kV/cm, 250 µs; 3 kV/cm, 100 µs; 3 kV/cm, 200 µs, respectively) (Adapted from Riske and Dimova (2005), Copyright 2005, with permission from Elsevier)

duration in the 50–200 µs range, and strength between 1 and 4 kV/cm. The deformation imposed to the vesicles is similar to that of low frequency AC fields. However, the presence of salt in the external medium imposes an additional deformation, a flattening of the vesicle sides along the field, see Fig. 4 (Riske and Dimova 2006). Thus, for $\lambda_{in}/\lambda_{ex} < 1$ an oblate-like spherocylinder is observed and for $\lambda_{in}/\lambda_{ex} > 1$ the vesicles assume either a prolate shape in the absence of external salt or a prolate-like spherocylindrical shape when salt is present in the vesicle exterior. The maximum shape deformation is usually attained toward the end of the pulse, and the dynamics of vesicle deformation during the pulse can only be resolved with a fast camera acquisition system, as for instance in (Riske and Dimova 2005), where 50 µs resolution was employed.

Characteristic Relaxation Times

The characteristic relaxation times for the vesicle deformation after the end of the pulse depend on the membrane material properties and on the phenomena stimulated by the pulse (Riske and Dimova 2005). Weak fields (below the electroporation

threshold, see Eqs. 1 and 2) induce only a mild deformation due to membrane stretching. After the end of the pulse, the vesicle quickly relaxes back to the initial shape with characteristic time $\tau_1 \sim 0.1$ ms by releasing the acquired membrane tension through shear in the membrane. Thus, τ_1 is related to the membrane tension σ acquired at the end of the pulse and to the surface viscosity of the bilayer, such that $\tau_1 \sim \eta_s/\sigma$. When DC pulses strong enough to reach the poration threshold of the membrane are applied to spherical vesicles, the deformation induced is stronger and macropores with diameters of few micrometers may open. These pores can be clearly visualized with phase contrast when glucose/sucrose asymmetry is employed (submicron pores may be present but cannot be visualized optically; see also "▶ Electropore Energy and Thermodynamics," "▶ Pore Lifetime and Permeabilization Lifetime in Models," "▶ Phospholipid Head Group Dipoles and Electropore Formation," "▶ Membrane Permeabilization Lifetime in Experiments," "▶ Electroporation and Electropermeabilization," "▶ Lipid Electropore Lifetime in Molecular Models," "▶ Lipid Electropore Geometry (Radius, Volume, Shape, Size) in Molecular Models," and "▶ Experimental Determination of Lipid Electropore Size"). After the pulse, the vesicle deformation relaxation is about two orders of magnitude slower ($\tau_2 \sim 10$ ms) than when no macropores are present. This second characteristic time τ_2 is related to pore closing time (see more details in the following section), which is set by the pore edge tension γ and the membrane surface viscosity η_s, such that $\tau_2 \sim \eta_s r/2\gamma$, where r is the pore radius. When the pulses are applied to GUVs with some excess area (seen by their shape fluctuation in the absence of applied field), a third and much longer relaxation time can be detected, $\tau_3 \sim 0.1$–1 s, depending on the excess area available. This slow time reflects the dynamics of volume displacement around the deformed vesicle of radius R. It is associated with shape fluctuations and entails contributions from the medium viscosity η (of sucrose/glucose solutions), the membrane bending rigidity κ and the vesicle reduced volume ($v \approx 0.95$–0.99 for deflated quasispherical vesicles), such that $\tau_3 \sim 4\pi\eta R^3/(3\kappa\,(v-1))$. These relaxation times quantified from the time dependence of the aspect ratio a/b of prolate vesicles are illustrated in Fig. 4.

Curiously, strong (even excessive) vesicle deformation with aspect ratios a/b up to 10 can also be observed (Sadik et al. 2011). Several theoretical studies were motivated by the experimental results on vesicle deformation induced by electric fields, in which the vesicle relaxation dynamics was considered using a droplet-based model, which yielded a way of deducing the initial tension of the vesicle and the membrane bending rigidity.

Electroporation of GUVs

Electric fields strong enough to build a transmembrane potential above a critical value ($V_m > V_c$, see Eq. 1 and section "Electrical Properties of Bilayers") cause opening of macropores in GUVs. Submicroscopic pores are also expected to open, but they cannot be resolved with optical microscopy. The macropores formed have a diameter of few micrometers and can be easily detected with phase contrast and

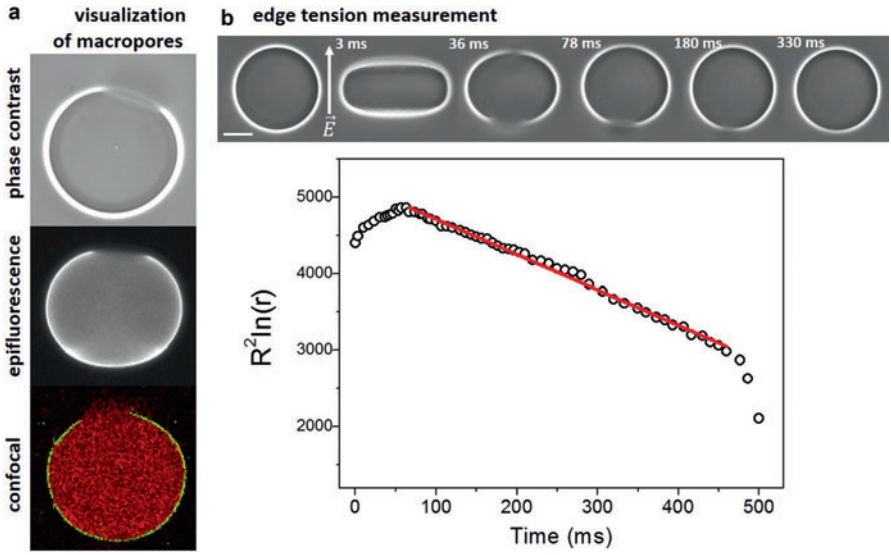

Fig. 5 (**a**) Detection of pulse-induced macropores with phase contrast (*top*: GUV with sucrose/glucose asymmetry), epifluorescence (*middle*: GUV labeled with membrane probe), and confocal microscopy (*bottom*: GUV labeled with green membrane probe and encapsulating a red aqueous soluble dye). The diameters of the vesicles are about 40 μm. (**b**) Electroporation used to measure edge tension following the approach in Portet and Dimova (2010). *Top*: sequence of images of a POPC GUV during and after application of a DC pulse (3 kV/cm, 150 μs). *Bottom*: dynamics of pore closure with linear fit to the slow pore closure regime which gives for the edge tension $\gamma = 25$ pN for this particular GUV

fluorescence microscopy (see Fig. 5). The pore lifetime entails four stages (Brochard-Wyart et al. 2000): (i) pore growth, (ii) stabilization, (iii) slow pore closure in a quasistatic leak-out regime, and (iv) fast pore closure. The third and longer stage is governed by the medium viscosity η and by the pore edge tension γ. The edge tension can be easily extracted from linear fits of the dynamics of the radius of the pore r in a vesicle of radius R according to the following equation (Brochard-Wyart et al. 2000):

$$R^2 \ln(r) = -\frac{2\gamma}{3\pi\eta} t + C \tag{3}$$

where C is a constant and t is the time. Phospholipid bilayers in the fluid phase have $\gamma \sim 30$ pN, and this value increases typically twice in the presence of cholesterol at physiologically relevant concentrations (Portet and Dimova 2010). The typical lifetime of micrometer-sized pores is of about tens of milliseconds.

In fluid vesicles, DC pulses can occasionally induce macropores that remain stably open or even never reseal, leading to vesicle destabilization and collapse. Stable and long-lived pores can be observed in the presence of cone-shaped molecules in the bilayer which lead to reducing the edge tension (Karatekin et al. 2003) or in the

presence of hydrogel polymers (agarose) which can physically hinder the pore closure (Lira et al. 2014), see Fig. 6. Interestingly, pores opened across cellular membranes might also never reseal due to physical obstruction of intracellular material leaking out. When DC pulses are applied to GUVs containing a large fraction of negatively charged lipids (POPC:POPG 1:1), vesicle burst/collapse is often observed (Riske et al. 2009). After the end of the pulse, macropores can be detected, but instead of resealing as in the case of zwitterionic membranes, the pores often continue to open and the whole vesicle collapses into a network of lipid tubes, as shown in Fig. 6. Therefore, the presence of negatively charged lipids has an impact on membrane stability, most probably by reducing the edge tension significantly.

The mechanical, rheological, and electrical properties of membranes in the gel phase (for example, sphingomyelin or dipalmitoylphosphatidylcholine – at room temperature) differ significantly from those of fluid lipid membranes shown above. Some of them are summarized in Table 1. These differences introduce new features in the response of gel-phase membranes to electric fields. Because of the high bending rigidity, gel-phase vesicles relax much faster after electrodeformation induced by electric pulses. The critical transmembrane potential leading to the poration of gel-phase vesicles is several times higher compared to that of fluid membranes (Knorr et al. 2010), one of the reasons being the larger membrane thickness, which implies that pulses of much higher field strength are needed to porate them. The resealing of macropores in gel-phase membranes is arrested. Upon poration, gel-phase GUVs develop cracks which do not reseal within minutes (Knorr et al. 2010).

Electrofusion of GUVs

If electroporation is induced in the contact area between two neighboring (fluid) GUVs, vesicle fusion may occur. Exposing the GUVs to AC fields prior to application of porating DC pulses can bring vesicles together (see Fig. 3b), thus increasing the likelihood of vesicle fusion. The first step in the fusing process after application of the pulse is the formation of a fusion neck from the merge of the two pore edges in the membranes of the adjacent GUVs. The size of this fusion neck can be followed with fast video microscopy (Haluska et al. 2006). In some cases, several fusion necks can form (see Fig. 7 for an example). The dynamics of neck growth involves two processes, as can be clearly seen in Fig. 7: a fast neck opening (with a velocity of a few cm/s) within the first millisecond, followed by a much slower increase in the fusion neck that requires a few seconds to finally result in a single vesicle. The initial fast process is driven by the dissipation of the high membrane tension acquired in the fusion neck zone, and it is thus dependent on the same parameters as the fast relaxation dynamics of nonporated vesicles ($\tau_{fast} \sim \eta_s/\sigma \sim 0.1$ ms). After the release of the membrane tension, the expansion of the fusion neck slows down by orders of magnitude and is then dictated by the slow mixing of the inner volumes of the two initial vesicles and by expelling of fluid around the fusion neck which is governed by the membrane bending stiffness κ, in a similar way as the long relaxation dynamics τ_3 of fluctuating GUVs ($\tau_{slow} \sim \eta\ \Delta V/\kappa \sim 10$ s).

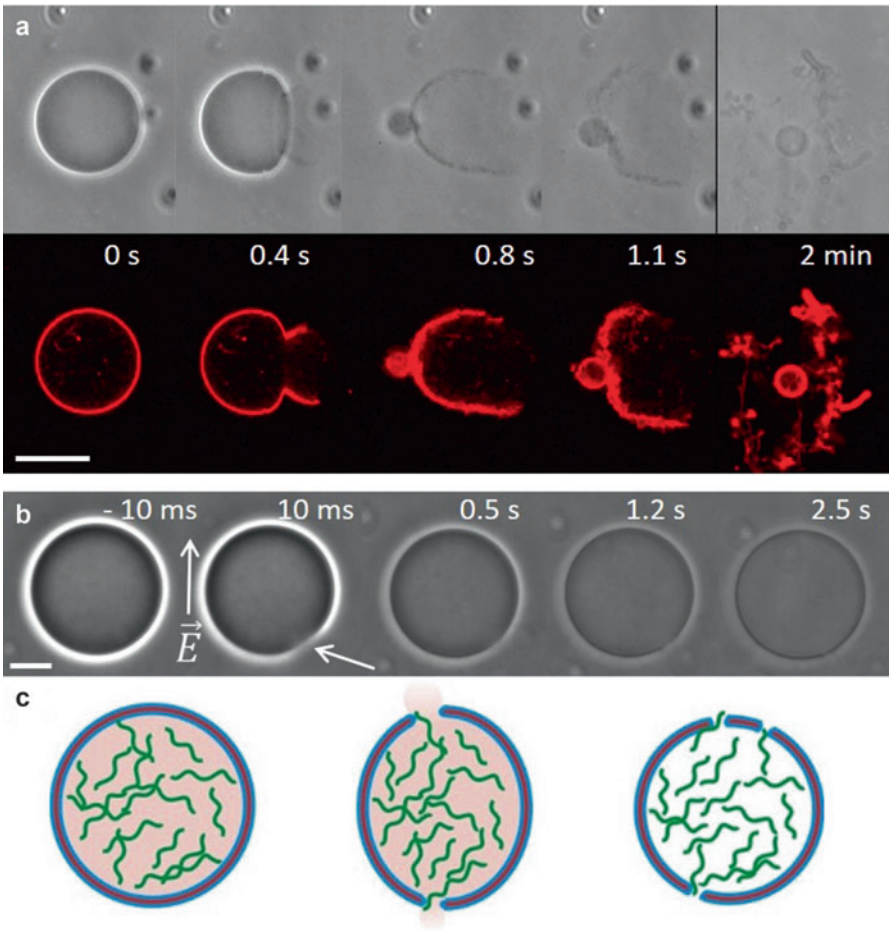

Fig. 6 – (**a**) Pulse-induced bursting of a POPC:POPG 1:1 GUV. The images were obtained with phase contrast (*top*) and confocal microscopy (*bottom*). The DC pulse applied was 3 kV/cm and 150 μs. The scale bar corresponds to 25 μm. Reproduced from (Riske et al. 2009) with permission from The Royal Society of Chemistry. (**b**) A POPC GUV encapsulating agarose gel is shown before, during, and after application of a DC pulse (3 kV/cm, 150 μs). The *arrow* points to the opened macropore. The scale bar corresponds to 20 μm. (**c**) Cartoon showing the physical obstruction of agarose polymer hindering pore resealing after electroporation. The inner solution (*pink*) leaks out and the vesicle looses contrast (**b**–**c** are adapted from (Lira et al. 2014) Copyright 2014, with permission from Elsevier)

From a more practical viewpoint, electrofusion of GUVs can be used to initiate targeted mixing of either their encapsulated content or their membranes. Vesicles encapsulating two different components or of two distinct membrane composition (and labeled differently to distinguish them) can be brought together either by AC fields, via micromanipulation with glass capillaries of micrometer diameter (micropipettes) or using microfluidic devices. After application of a strong DC pulse,

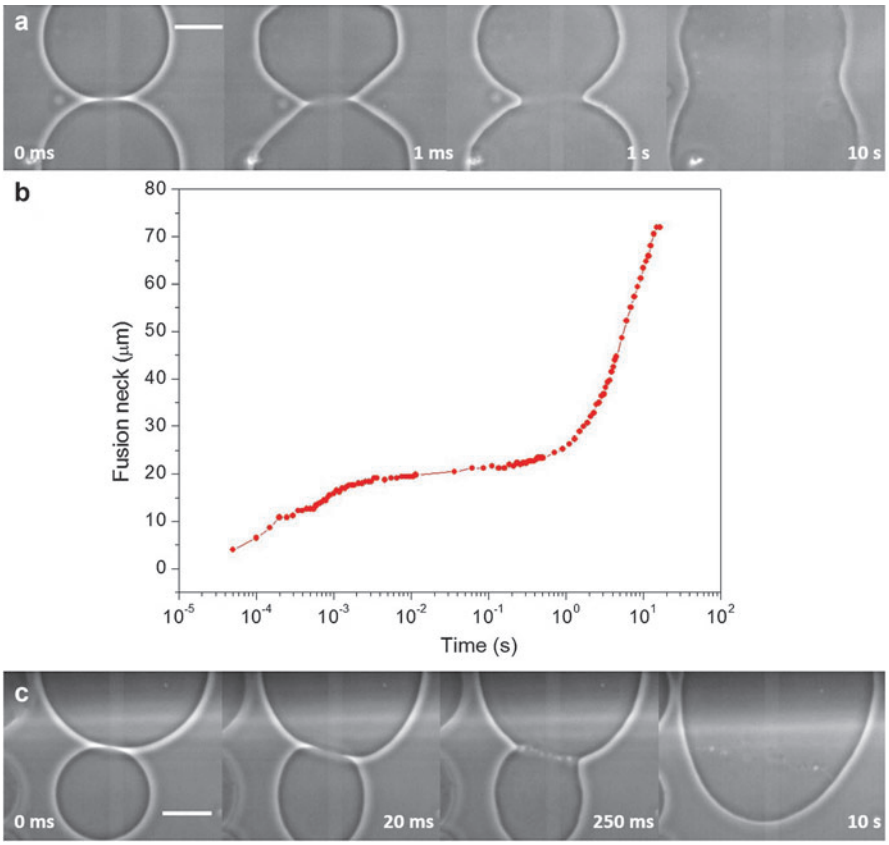

Fig. 7. (**a**) Electrofusion of two egg-PC GUVs. (**b**) Dynamics of the size of the fusion neck. (**c**) Electrofusion of two egg-PC GUVs through several fusion necks. The scale bars represent 20 μm (Adapted from Haluska et al. (2006), Copyright 2006, National Academy of Sciences)

vesicle fusion may occur thus (i) initiating the reaction of the solutes in the two components encapsulated in the two vesicles or (ii) mixing of the membranes of the two vesicles. An example for using vesicle electrofusion as a microreactor is the synthesis of quantum-dot-like CdS nanoparticles in the closed compartment of a fused vesicle couple (Yang et al. 2009) as illustrated in Fig. 8. In this case, two GUVs, one loaded with Na_2S and the other loaded with $CdCl_2$, are fused. The product of the reaction, quantum-dot-like CdS nanoparticles, can be visualized under laser excitation as a fluorescent bright spot in the fusion zone (see last image in Fig. 8b). This method could be especially suitable for the online monitoring of several physicochemical processes such as photosynthesis, enzyme catalysis, and photopolymerization. On the other hand, fusing of two vesicles with known surface area and lipid composition can be used to produce GUVs with precise multicomponent lipid composition (Bezlyepkina et al. 2013). This is important

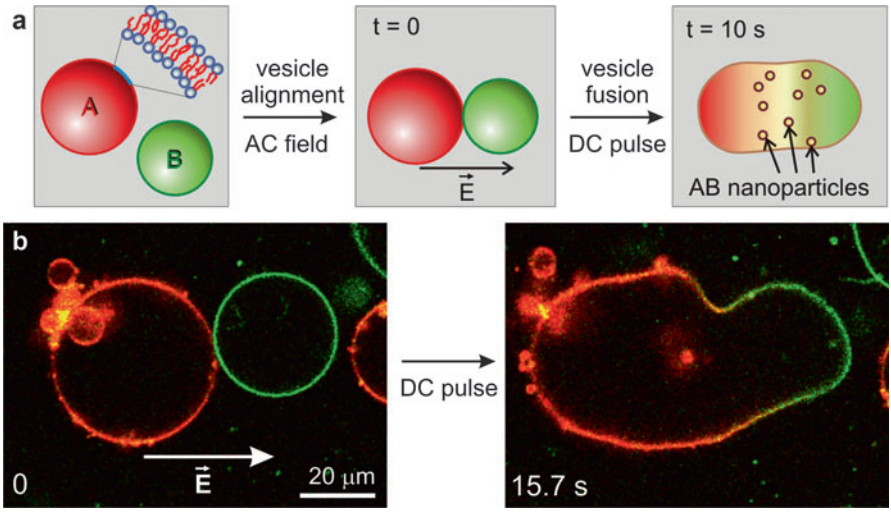

Fig. 8. Electrofusion of giant vesicles as a method for nanoparticle synthesis. (**a**) Schematic illustration of the electrofusion protocol: Two populations of vesicles containing reactant A or B are mixed (in A- and B-free environment). The vesicles are subjected to an AC field to align them in the direction of the field and bring them close together. A DC pulse initiates the electrofusion of the two vesicles and the reaction between A and B proceeds to the formation of nanoparticles encapsulated in the fused vesicle. (**b**) Confocal cross-sections of giant vesicles loaded with Na_2S (*red*) and $CdCl_2$ (*green*) undergoing electrofusion. After fusion (*right*), fluorescence from the product is detected in the interior of the fused vesicle. The time after applying the pulse is indicated on the micrographs (Reproduced from Yang et al. (2009) with permission from John Wiley and Sons)

because GUVs grown from lipid mixtures can exhibit widely different individual composition, depending on the individual vesicle history. For example, before observation, a phase-separated vesicle may have budded in the region of one of the domains and the two daughter vesicles would then have attained compositions that are very different from that of the mother vesicle. Indeed, in samples with compositions belonging to the region of coexistence of two fluid phases, one often finds vesicles that are not phase-separated. Particularly strong deviations in the vesicle composition are observed for multicomponent lipid mixtures that are not fully miscible at the temperature of observation. To overcome this problem, electrofusion of two vesicles made of two different fully miscible lipid mixtures can be employed (Bezlyepkina et al. 2013).

Conclusion

Electric fields induce a variety of effects on GUVs. Moderate fields cause shape deformation and vesicle movement/alignment. Stronger fields are able to induce electroporation and membrane fusion if vesicles are in close contact. These

phenomena and their dynamics depend on the vesicle state (e.g., its tension and excess area) and on the material properties of the lipid bilayer, such as membrane bending stiffness, surface viscosity, edge tension, capacitance, and poration threshold. Here it was shown that AC and DC fields can be used to manipulate GUVs, for instance to pull out excess area stored in shape fluctuations, and to extract membrane properties such as bending stiffness and edge tension, and how these properties change with membrane composition. Several other applications can be envisaged for model systems in the presence of electric fields. For instance, more complex membranes could be used for obtaining GUVs (e.g., with complex biological lipid mixtures, with specific membrane proteins incorporated, and with a cytoskeleton which provides mechanical stability to the vesicle). This will allow the study of systems that capture better the complexity of real cells.

Acknowledgment K.A.R. acknowledges the financial support of FAPESP.

Cross-References

- ▶ Critical Electric Field and Transmembrane Voltage for Lipid Pore Formation in Experiments
- ▶ Critical Electric Field and Transmembrane Voltage for Lipid Pore Formation in Molecular Models
- ▶ Electric Pulse Parameters Affecting Electroporation Treatment Outcome
- ▶ Electroporation and Electropermeabilization
- ▶ Electropore Energy and Thermodynamics
- ▶ Experimental Determination of Lipid Electropore Size
- ▶ Gene Delivery by Electroporation In Vitro: Mechanisms
- ▶ Lipid Electropore Geometry (Radius, Volume, Shape, Size) in Molecular Models
- ▶ Lipid Electropore Lifetime in Molecular Models
- ▶ Membrane Permeabilization Lifetime in Experiments
- ▶ Molecular Transmembrane Transport with Giant Unilamellar Vesicles (GUVs)
- ▶ Nucleic Acid Electrotransfer in Mammalian Cells: Mechanistic Description
- ▶ Phospholipid Head Group Dipoles and Electropore Formation
- ▶ Pore Lifetime and Permeabilization Lifetime in Models
- ▶ Pulsed Electric Fields Treatment of Biological Suspensions

References

Aranda S, Riske KA, Lipowsky R, Dimova R (2008) Morphological transitions of vesicles induced by alternating electric fields. Biophys J 95(2):L19–L21

Bezlyepkina N, Gracià RS, Shchelokovskyy P, Lipowsky R, Dimova R (2013) Phase diagram and tie-line determination for the ternary mixture DOPC/eSM/cholesterol. Biophys J 104 (7):1456–1464

Brochard-Wyart F, de Gennes PG, Sandre O (2000) Transient pores in stretched vesicles: role of leak-out. Physica A 278(1–2):32–51

Dimova R (2014) Recent developments in the field of bending rigidity measurements on membranes. Adv Colloid Interface Sci 208:225–234. doi:10.1016/j.cis.2014.03.003

Dimova R, Bezlyepkina N, Jordo MD, Knorr RL, Riske KA, Staykova M, Vlahovska PM, Yamamoto T, Yang P, Lipowsky R (2009) Vesicles in electric fields: some novel aspects of membrane behavior. Soft Matter 5(17):3201–3212

Dimova R, Riske KA, Aranda S, Bezlyepkina N, Knorr RL, Lipowsky R (2007) Giant vesicles in electric fields. Soft Matter 3(7):817–827

Gracià RS, Bezlyepkina N, Knorr RL, Lipowsky R, Dimova R (2010) Effect of cholesterol on the rigidity of saturated and unsaturated membranes: fluctuation and electrodeformation analysis of giant vesicles. Soft Matter 6(7):1472–1482. doi:10.1039/b920629a

Haluska CK, Riske KA, Marchi-Artzner V, Lehn JM, Lipowsky R, Dimova R (2006) Time scales of membrane fusion revealed by direct imaging of vesicle fusion with high temporal resolution. Proc Natl Acad Sci U S A 103(43):15841–15846

Harbich W, Helfrich W (1979) Alignment and opening of giant lecithin vesicles by electric-fields. Z Naturforsch, A: Phys Sci 34(9):1063–1065

Karatekin E, Sandre O, Guitouni H, Borghi N, Puech PH, Brochard-Wyart F (2003) Cascades of transient pores in giant vesicles: line tension and transport. Biophys J 84(3):1734–1749

Knorr RL, Staykova M, Gracia RS, Dimova R (2010) Wrinkling and electroporation of giant vesicles in the gel phase. Soft Matter 6(9):1990–1996

Lira RB, Dimova R, Riske Karin A (2014) Giant unilamellar vesicles formed by hybrid films of agarose and lipids display altered mechanical properties. Biophys J 107(7):1609–1619. doi:10.1016/j.bpj.2014.08.009

Portet T, Dimova R (2010) A new method for measuring edge tensions and stability of lipid bilayers: effect of membrane composition. Biophys J 99(10):3264–3273

Rawicz W, Olbrich KC, McIntosh T, Needham D, Evans E (2000) Effect of chain length and unsaturation on elasticity of lipid bilayers. Biophys J 79(1):328–339

Riske KA, Dimova R (2005) Electro-deformation and poration of giant vesicles viewed with high temporal resolution. Biophys J 88(2):1143–1155

Riske KA, Dimova R (2006) Electric pulses induce cylindrical deformations on giant vesicles in salt solutions. Biophys J 91(5):1778–1786

Riske KA, Knorr RL, Dimova R (2009) Bursting of charged multicomponent vesicles subjected to electric pulses. Soft Matter 5:1983–1986

Sadik MM, Li J, Shan JW, Shreiber DI, Lin H (2011) Vesicle deformation and poration under strong dc electric fields. Phys Rev E 83(6):066316

Simons K, Ikonen E (1997) Functional rafts in cell membranes. Nature 387(6633):569–572

Walde P, Cosentino K, Engel H, Stano P (2010) Giant vesicles: preparations and applications. Chem Bio Chem 11(7):848–865

Yang P, Lipowsky R, Dimova R (2009) Nanoparticle formation in giant vesicles: synthesis in biomimetic compartments. Small 5(18):2033–2037